Journal of
Chemical Engineering & Process Technology

Akl et al., J Chem Eng Process Technol 2013, 4:4
DOI: 10.4172/2157-7048.1000154

Research Article Open Access

Removal of Iron and Manganese in Water Samples Using Activated Carbon Derived from Local Agro-Residues

Magda A. Akl*, AbdElFatah M. Yousef and Sameh AbdElnasser

Chemistry department, Faculty of Science, Mansoura University, Mansoura, Egypt

Abstract

Three olive stones-derived activated carbons (ACOS) with different chemical characteristics, appropriate for the removal of iron and manganese in groundwater are prepared. The steam activated carbon is obtained from carbonized olive stones in the presence of nitrogen in the temperature range from 700 to 900°C and modified by HNO_3 and ammonium persulphate. The structure of the activated carbons was characterized by N_2 adsorption at 77 K, scan electron microscopy and FTIR. B.E.T and α-methods are used to deduce the effective surface areas. The parameters (such as initial pH, temperature, etc) affecting the adsorption capacity of ACOS toward iron and manganese cations removal from aqueous solutions are investigated using batch experiments. The study of kinetic models including pseudo first order and pseudo second-order are carried out. Langmuir adsorption isotherm is investigated. Equilibrium adsorption data fitted the Langmuir adsorption isotherm well with R^2>0.9908. The maximum adsorption capacities of ACOS for the removal of iron and manganese cations are calculated. The results obtained revealed that the sample activated by HNO_3 has the highest adsorption capacity followed by ammonium persulphate and steam activated samples. The mechanism of adsorption is proposed.

Keywords: Activated carbons; Adsorption; Iron; Manganese; Groundwater; HNO_3; Ammonium persulphate; Langmuir isotherm

Introduction

Ground water is the major source of drinking water in rural and semi-urban areas of Egypt. Both iron and manganese are common contaminants in groundwater, in concentrations exceeding 10 µg/L but they are rarely present in contaminations exceeding 1.0 g/L [1]. The World Health Organization (WHO) has set a guideline value of 0.3 mg/L of iron and 0.05 mg/L of manganese in drinking water [2], and many of the countries, including Egypt, have adopted this value in their national drinking water standards. In the Delta district of Egypt, where Dakahlia Governorate is located, a substantial part of groundwater used for potable uses shows contamination significantly exceeding the maximum contaminant level (MCL). The presence of high concentrations of iron and manganese in water causes economic and technological problems. On contact with air, they precipitate a dark sludge with influences the development of ferruginous and manganese bacteria on walls of pipes enhancing thus the corrosion of the pipes [3,4]. Manganese is also toxic to the brain resulting in neurological disorder similar to Parkinson's disease [5,6]. Although iron is an essential mineral for human, its presence in ground water above a certain limit makes the water un-usable for aesthetic considerations such as metallic taste, odour, staining of laundry and plumping fixtures.

A number of specialized processes have been developed for the removal of metals from water and waste discharges. These unit operations include: chemical precipitation [7,8], coagulation/flocculation [9,10], ion exchange/solvent extraction [11,12], cementation [13,14], complexation [15,16], electrochemical operation [17], biological operations [18], evaporation [19], filtration [20], membrane processes[21] and adsorption [22-26].

Adsorption of heavy metals on activated carbons (ACs) and modified ACs proved to be the most efficient technique in this application. It is recommended to use low cost precursors that are available in large amount, renewable and contain high carbon content and low inorganic content. These requirements are found in many agricultural wastes [25]. Olive stones are agricultural waste which has been widely used for the preparation of ACs [27,28].

The objective of the present investigation is the preparation of AC developed from olive stones and to modify the surface of these carbons by surface oxidation with concentrated nitric acid and ammonium persulfate. The textural properties and the chemistry of the surface of the carbons prepared were determined. The adsorption of Mn (II) and Fe (III) from their aqueous solution, at different conditions of solution volume, adsorbent mass, solution concentration, pH and temperature, kinetic and equilibrium adsorption were performed.

Materials and Methods

Materials

The chemicals used HCl, HNO_3, $(NH_4)2S_2O_8$), NaOH and standard stock of iron ($FeCl_3$), manganese ($MnCl_2$) were of analytical grade. Stock solutions containing 1000 mg/l of $Fe_2(SO_4)_3 12H_2O$ and 1000 mg/l of $MnCl_2$ by dissolving the calculated amounts in doubly distilled water.

Preparation of the activated carbons

The activated carbon C was prepared by carbonizing clean dry crushed olive stones (0.4-0.6 mm) in nitrogen atmosphere at 450°C, followed by gasification with steam at 900°C to a burn off=29%. Details of preparation are reported elsewhere [25]. Modification of steam activated carbon "C" was carried out by oxidation with 65% nitric acid to get HNO_3-modified carbon "C1". Oxidation with ammonium persulphate of carbon C was also carried out to get persulphate-modified carbon "C2" Details of procedures are given elsewhere [28].

***Corresponding author:** Prof. Magda A. Akl, Chemistry Department, Faculty of Science, Mansoura University, Mansoura, Egypt, E-mail: magdaakl@yahoo.com

Received April 09, 2013; **Accepted** April 23, 2013; **Published** April 25, 2013

Citation: Akl MA, Yousef AM, AbdElnasser S (2013) Removal of Iron and Manganese in Water Samples Using Activated Carbon Derived from Local Agro-Residues. J Chem Eng Process Technol 4: 154 doi:10.4172/2157-7048.1000154

Copyright: © 2013 Akl MA, et al. This is an open-access article distributed under the terms of the Creative Commons Attribution License, which permits unrestricted use, distribution, and reproduction in any medium, provided the original author and source are credited.

Characterization of the activated carbons

The adsorption of nitrogen at 77 K was studied using a conventional volumetric apparatus. Prior to adsorption, the carbon sample was degassed at 473 K under a reduced pressure of 10^{-5} Torr. The adsorption was followed until a relative pressure p/po=0.95 and the desorption was continued until the closure of the hysteresis loop.

Scanning electron microscopy of activated carbons was examined using the SEM (JEOL-JEM-100S) under the following conditions: The samples were prepared by sprinkling the powder lightly onto a double-sides adhesive tape which was mounted on SEM specimen stub. The edges of the double-sided tape were printed with gold. Micrographs were obtained in a secondary electron imaging mode using a potential difference of 25 KV. SEM observations were carried out at magnification of 400x. Representative sections of surfaces were recorded and developed on monochrome paper (IL Ford FP4).

A Fourier transform infrared (FTIR) spectrometer (Perkin-Elmer) model 1430 was used to detect the IR-observable functional groups on the carbon surface, in the wave number range 4000-400 cm^{-1}. The samples were first mixed with KBr and then pressed into pellets. The KBr pellet contains 0.5 wt% carbon.

Adsorption of iron and manganese

Batch experiments were carried out by shaking a stopper flasks containing specific concentration of Fe^{3+} or Mn^{2+} cations solution and specific amount of ACOS at 80 rpm for desirable time, temperature and initial pH. The suspensions were then filtered and the filtrates were analyzed using flame atomic absorption spectrophotometer (Perkin-elmer model 2380). The pH values of suspensions were adjusted with dilute HCl or NaOH solution. The experiments were carried out by varying the initial metal ion concentration, contact time, amount of the adsorbent, pH of the initial suspension.

Results and discussion

Characterization of activated carbons

Textural properties: The surface area and porosity of carbons are prominent factors in determining their adsorption capacities [29]. The textural properties of solids are conventionally determined from the adsorption of nitrogen at 77 K and the adsorption data are usually analyzed by the application of the BET equation [30].

The adsorption of nitrogen by the carbons investigated was found to be relatively rapid with the equilibrium attained within 25 min indicating that the adsorption is not controlled by activated diffusion encountered in ultrafine pores and meanwhile refers to the accessibility of the entire pore structure to the nitrogen molecules [24]. Figure 1 depicts the nitrogen adsorption isotherms measured at 77 K for the carbons C, C1 and C_2.The isotherms of carbon C is mainly type I according to the BDDT classification with no hysteresis loop [31], this isotherm is also characterized by very steep initial portion and gave the highest BET-C constant (Table 1).

The isotherms of carbon C1 and C2 show mixed characteristics of type I and type Π, they are less steep and exhibited closed hysteresis loops. The nitrogen adsorption data fitted very well the BET equation. The linear BET plots are shown in figure 2. The surface areas SBET (m^2/g) were calculated and the total pore volume VT (ml/g) were read from the volume of nitrogen adsorbed at P/P0 = 0.95. Included also in table 1 are the BET-C constant and the mean pore radius r (nm), calculated from the relationship: $r=(2V_T(ml/g)*10^3)/S_{BE}T\ (m^2/g)$.

More knowledge on the texture of the carbons investigated could be obtained by considering the α-method [32] in analyzing the nitrogen adsorption results. The application of the α-method has been performed using the standard data reported [33].

This method is considered as an independent method for the determination of the specific surface area S_α (m^2/g) from nitrogen adsorption data. The method allows also the determination of some important textural parameters. These parameters are the area of micropores S_m^α and the area of non-micropores S_n^α. The volumes of micropores and of non-micropores V_m^α and V_n^α have been also determined. Figure 3, shows the α-plots of C, C_1 and C_2. The textural parameters determined by the α-method are listed also in table 1.

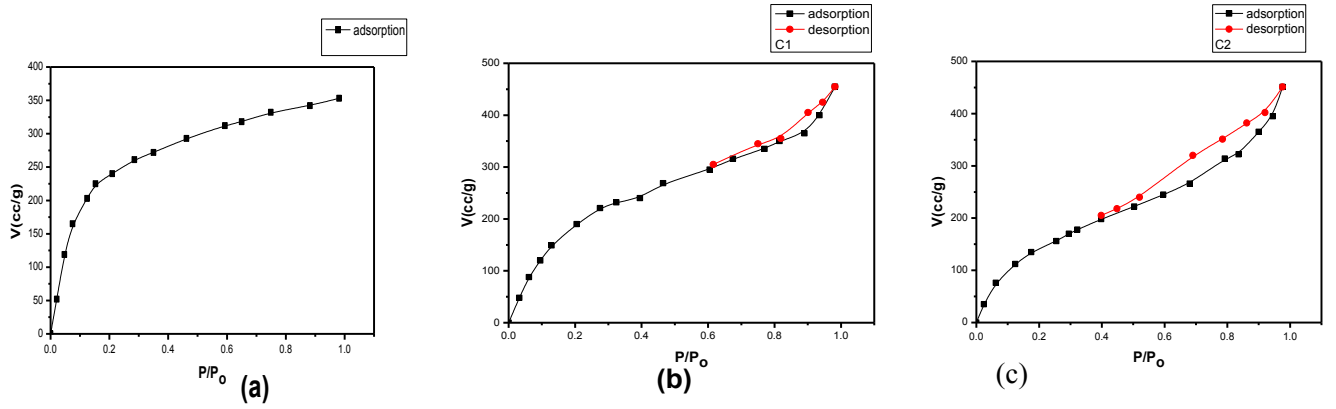

Figure 1: The nitrogen adsorption isotherms at 77 K of (a) C; (b) C1 and (c) C2.

Carbon	$S_{BET}m_2/g$	V_T m/g	r nm	BET-C constant	S_α m^2/g	S^α_n m^2/g	S_m^α m_2/g	V_n^α ml/g	V_m^α ml/g	V_m^α/VT %
C	831.3	0.547	1.32	25	812	136	676	0.136	0.401	73.3
C1	729.6	0.705	1.93	18.5	740	385	335	0.39	0.25	35.5
C2	576	0.699	2.43	11	525	265	260	0.599	0.1	14.3

Table 1: Textural characteristics of the carbons investigated.

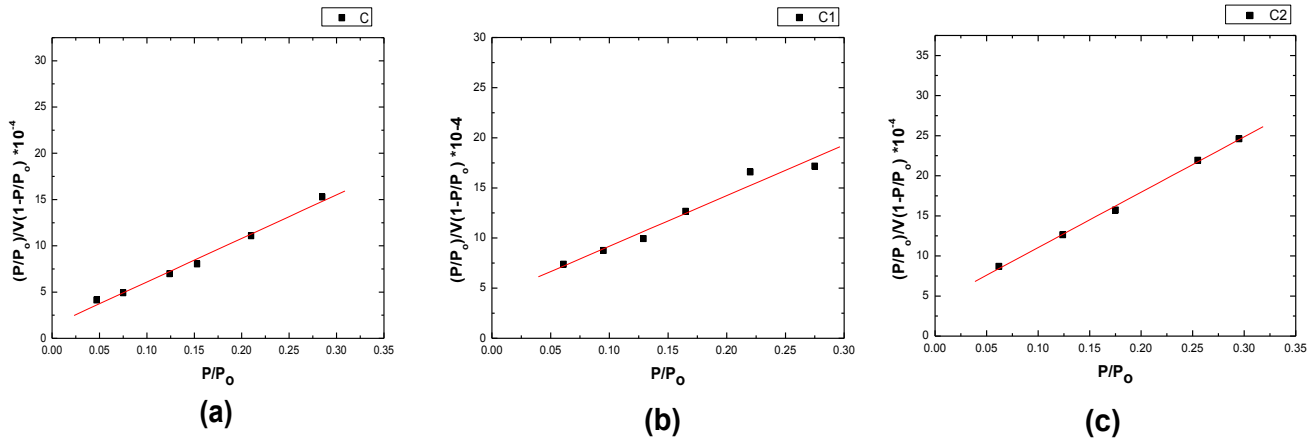

Figure 2: Linear BET plots of nitrogen adsorption at 77 K by (a) C; (b) C1 and (c) C2.

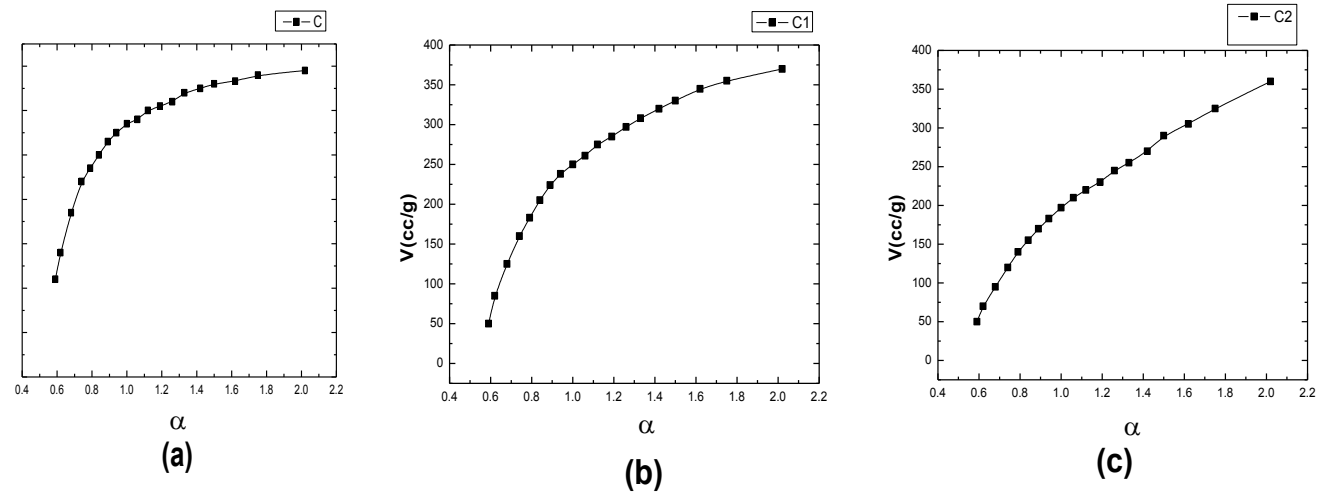

Figure 3: The α plots of nitrogen adsorption at 77 k of (a) C; (b) C1 and (c) C2.

Table 1 depicts: (i) comparable surface areas are obtained from the BET-method and the α-method. This may be taken as an evidence for the reliability of the measurements. (ii) The surface area of the un-oxidized activated carbon is higher than those of the oxidized derivatives. (iii) The total pore volume of the un-oxidized carbon C is lower than those of the oxidized carbons C1 and C2. This could be attributed to the pore widening brought about by oxidation. Evidently r of carbon C was calculated to be 1.32 nm, where as r of C1 was calculated to be 1.93 nm and r of C2 was found to be the largest , i.e=2.43 (nm). Included also in table 1 are the ratio V_m^{α}/V_T, the values obtained may be taken as a support for the pore widening due to oxidation of activated carbons. Thus, the ratio was 73.3% for C, 35.5% for C1 and dropped to 14.3%. (iv) The textural changes depend among other factors on the oxidizing agent used.

The scanning electron microscopy: The scanning electron microscopy images gave insight into the olive stone structure with respect to its shape. The dark areas are macro pores and the pale grey areas are due to the carbon matrix. Figure 4, represents the morphology of the resulting activated carbon prepared via physical (C) and chemical (using HNO_3, C1) activation methods, respectively. It can be clearly seen that physical and chemical activations show some changes in the surface of the particles after activation. The different pore structures of the activated carbon prepared from either physical (using nitrogen as activating agent) or chemical (using HNO_3) activation are observed, which depend upon different reaction mechanisms. Figure 4, depicts two pictures (a) for physically activated carbon (C) and (b) for HNO_3 activated carbon (C1). In this concern, the sample (a) activated by N_2 gas indicated that the carbon matrix are greater than the dark areas. This is referred to the nature of the micro pores resultant from the activated N_2 gas. Whereas, the dark areas are greater than the carbon matrix using HNO_3 as activator in chemical activation. This implies to the higher surface area of sample (b) due to mesopores as well as to micro-pores.

Also, this shows that the olive stone activated by HNO_3 have irregular carbon matrix. i.e. of different shapes and sizes. This was proved by nitrogen adsorption isotherms of activated olive stone which indicated that they were mainly micro pores only in physical activation and mixture from micro- and mesopores in chemical activation.

This may be explained by progressive changes in the surface of the cellular structure of the parent material with HNO_3 solution used as

shown in figure 4. The cellulose units are hydrolyzed by the acid and thus the main components of inter cellular wall are broken down to smaller structure.

Thus it is apparent that the external surface of olive stone is quite rough, consisting of cavities, cracks, and irregular protrusions.

Chemistry of the carbon surface: The chemistry of the surface of a carbon is more important than its textural properties in determining its adsorption from aqueous solution particularly when the adsorption involves interaction with the surface functional groups via ion exchange and/or complex formation which is most probably the case in adsorption of metal ions on activated carbons.

The chemistry of the carbon surface is attributed to the existence on the surface of carbon-oxygen functional groups of acid or basic character. The FTIR spectra of samples C, C1 and C2 (before and after adsorption of iron and manganese) have been recorded. Because the surface C-O groups, particularly those of acid type are the most important sites for the adsorption of heavy metals from their aqueous solutions [34], concentration is directed to such functional groups.

The recorded IR spectra (before adsorption of iron and manganese) depict\the existence of absorption bands at 1610 cm^{-1}, 1365-1330 cm^{-1} and 1100-1081 cm^{-1} for C,C1 and C2. These bands are assigned respectively to symmetric COO- vibration [35], stretching C-O of OH groups and ether type structure and phenolic or aliphatic OH [36]. The band 1710-1705 cm^{-1} is shown only for the oxidized carbons C1 and C2, the 1710-1705 cm^{-1} band is assigned to stretching C=O vibration of lactone, quinine and carboxylic acid [37] which are all of acid type. Based on this, the existence, absence or shift in the location in the 1700-1750 cm^{-1} should be considered.

The FTIR spectra of C, C1 and C2 after the adsorption of Fe (III) showed the following changes: for carbon C, the disappearance of the 1610 cm^{-1} and the down ward shift of the 1340 cm^{-1} band to 1292 cm^{-1} and the appearance of a new band centered at 1207 cm^{-1} may account for Fe (III) interaction with the un-oxidized carbon C. A new band centered at 1750 cm^{-1} made its appearance upon Fe (III) uptake by this particular sample, taking in consideration that the FTIR spectra of carbon C, before iron adsorption did not show such band. This observation may be explained by the significant decrease in the pH of iron solution after equilibrium adsorption. It seems that Fe (III) can be adsorbed via ion exchange under certain circumstances. It has been reported on the carbon surface some C-O groups increased and new groups have appeared [38], possibly via a reaction such as

$$C+4Fe^{3+} + H_2O = CO_2 + 4Fe^{2+} + 4H^+.$$

For C1 and C2, the interaction with Fe (III) brought about a significant shift of the 1710 cm^{-1} band to 1740 cm^{-1} and the appearance of a new band centered at 1232 cm^{-1} together with the disappearance of the 1610 cm^{-1} and 1330 cm^{-1} bands.

The FTIR spectra of C, C1 and C2 after the adsorption of Mn (II) showed the following changes: for carbon C, the adsorption of Mn (II), the disappearance of 1340 cm^{-1} band and the shift of the 1610 cm^{-1} band to 1579 cm^{-1} may indicate the possible interaction of Mn (II) via complexation. For carbon C1, the interaction of Mn (II) with the surface was associated with the disappearance of the bands at 1610 cm^{-1} and 1330 cm^{-1} referring thus to the involvement of the corresponding groups in the interaction with Mn (II) via complexation. However the small shift of the 1710 cm^{-1} to 1705 cm^{-1} may not account for any mode of interaction. For C2, the interaction with Mn(II) proceeded also with the disappearance of 1610 cm^{-1} and 1365 cm^{-1} bands, together with the appearance of a band centered at 1207 cm^{-1} standing for =C-O symmetric stretching. These significant changes are related to the uptake of Mn (II) by carbon C2 via complex formation. It remains, here to exclude the uptake of Mn (II) via ion exchange process. The slight shift of the band at 1710 cm^{-1} upon Mn (II) interaction either with C1 or C2 may be taken as an evidence for this explanation. Evidence was shown by the negligible of the pH of Mn (II) solution prior to or after the adsorption.

The pH of the aqueous slurry of the carbon material provides a convenient indicator of the type and concentration of the chemical parameters of the ACs investigated. Table 2 reveals that (i) the surface pH of carbon C (8.5) indicate its surface basicity, i.e the basic functional groups on the surface of non-oxidized carbon are more dominating compared with those of the acid type. The same is also true, but to a less extent for C2 of surface pH=7.6. Steam activation at 950°C usually leads to the formation on the carbon surface of C-O groups of basic

carbon	Surface pH	pH zpc	Carboxyl (m.eq/g)	Lactonic (m.eq/g)	Phenolic (m.eq/g)	Carbonyl (m.eq/g)	Total (m.eq/g)
C	8.5	5.4	0.21	0.20	0.18	0.24	0.83
C1	5.2	4.4	1.00	0.89	1.02	1.55	4.45
C2	7.6	5.1	0.48	0.44	0.64	0.69	2.25

Table 2: Surface chemical parameters of the investigated carbons.

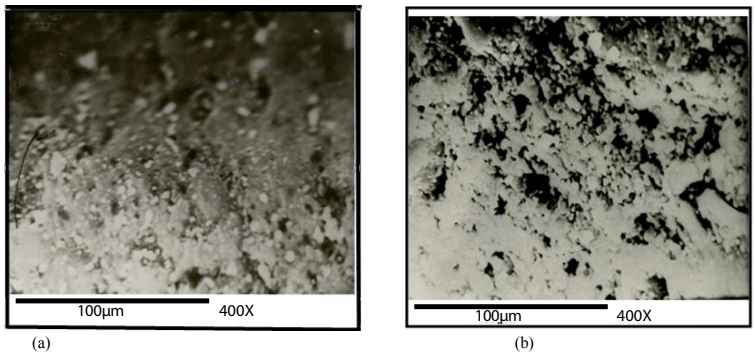

(a) (b)

Figure 4: Scanning electron micrographs of (a) steam activated carbon and (b) HNO_3-oxidized carbon at magnification of 400 x.

character [38]. Oxidation of steam activated carbon with nitric acid creates C-O groups of acid character decreasing thus the surface pH. Treatment with persulphate (C2) decreased the surface pH from 8.5 to 7.6, yet the strength of the acid was not high enough to turn over the surface pH in the acid range. Oxidation of carbon C with 45% nitric acid (C1) brought about this turn-over. Thus the surface pH of C1 was determined to be 5.2.

The pH of zero point charge pH pzc of C, C1, C2 were determined to be 5.4, 4.4 and 5.1, respectively (column 3 of Table 2). It seems that pH zpc is always lower than the corresponding surface pH, but both follow the same trend.

The surface acidic groups could be determined in (m.eq/g) by the selective neutralization with a series of bases of varying strength. $NaHCO_3$, Na_2CO_3, NaOH and $NaOC_2H_5$. $NaHCO_3$ neutralizes carboxylic groups where as those neutralized by Na_2CO_3 but not by $NaHCO_3$ are lactones. The weak acid groups neutralized by NaOH but not by Na_2CO_3 were postulated as phenols.

The reaction of $NaOC_2H_5$ is not considered as a true neutralization reaction since it did not involve change by H^+ or Na^+ ions.

The groups reacting with $NaOC_2H_5$, but not with NaOH, were suggested to be carbonyl groups [39]. Table 2 indicates that the concentration of the acids groups considerably increase with treatment with nitric acid with this increase depending of the acid strength used in the oxidation of the steam-activated carbon C. Table 2 reveals that:

i. The total surface acidity of HNO_3-oxidized carbon "C1" is the highest where as the non-oxidized activated carbon "C" measured the lowest surface acidity. Evidently carbon "C2" modified by oxidation with persulphate exhibited intermediate total surface acidity.

ii. Oxidation with persulphate was found to be associated with more than two fold increase with respect to the concentration of carboxyl and lactonic groups and about three fold increase in the concentration of both phenolic and carbonyl groups.

iii. On the other hand, oxidation with nitric acid brought about 5-6 fold increase in the concentration of the different types of the surface acid groups, compared with the non-modified carbon.

Adsorption of Fe (Ш) and Mn (П)

Effect of contact time: The effect of contact time is an important parameter in determining the equilibrium time that should be allowed for the maximum uptake of an adsorptive by a given adsorbent. Meanwhile, the determination of the uptake from an adsorptive at different time intervals permits the construction of an adsorption kinetic curve from which the adsorption rate constant and the order of the adsorption process could be obtained. The kinetics of Fe (Ш) and Mn (П) uptakes were followed using solutions of initial pH=6 and initial concentration of the adsorption solution=5 ppm and adsorbent dosage=0.010 g.

The kinetic adsorption curves of Fe (Ш) and Mn (П) by carbon C1 at 25°C are shown in figure 5. The data obtained show that the metal ion uptake by the oxidized carbon C1 increased with increasing contact time, with equilibrium being established in less than one hour. This equilibrium time was considered, but more time was allowed particularly in determining the equilibrium adsorption isotherms to ensure the attainment of equilibrium conditions.

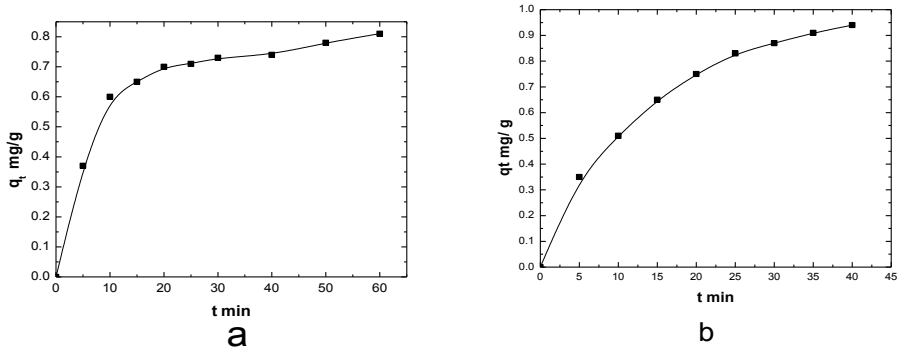

Figure 5: The kinetic adsorption curves of (a) Fe(Ш) and (b) Mn(П) by the activated carbon C1 at 25 ^{0}C.

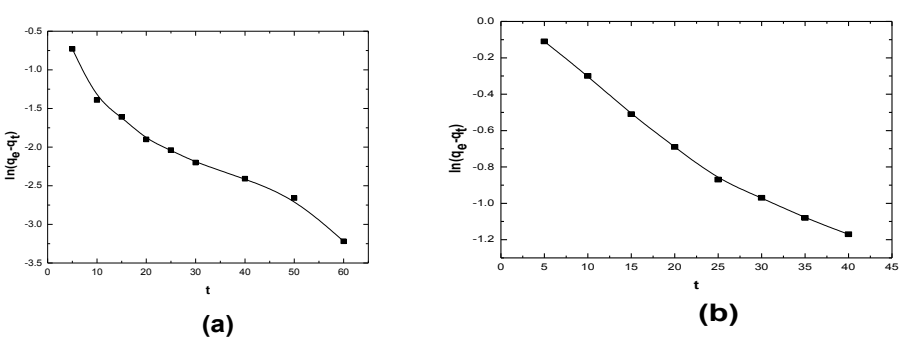

Figure 6: The sorption kinetics of Fe(Ш) and Mn(П) at initial concentration on oxidized carbon C1.

Usually the adsorption of heavy metal ions is analyzed using the Lagergren-first-order and pseudo-second order kinetic equations.

The Lagergren-first-order kinetic equation [40] is based on adsorbent capacity and may be written as

$$dq_t/dt = K_{1,ads}(q_e-q_t) \quad (1)$$

Where $K_{1,ads}$ (1/min) is the first-order sorption rate constant, q_e and q_t are the equilibrium uptake and the uptake at time t, respectively. Equation (1) can be integrated using the boundary conditions q_t=0 at t=0 to give

$$\ln (q_e-q_t)=\ln q_e - K_{1,ads}\, t \quad (2)$$

Thus if the adsorption kinetics obey the Lagergren-first-order kinetic equation, a plot of ln (qe-qt) versus t should result in a straight line. However, in many cases the Lagergren-first-order equation only fits the sorption kinetics over the first 15-20 min of the sorption process [41]. Figure 6 shows a fit of the sorption kinetics of Fe (Ш) and Mn (П) at initial concentration on oxidized carbon C1.

The pseudo-second-order kinetic equation [42] is, also based on the sorption capacity of the sorbent and is given by

$$dq_t/dt = K_{2,ads}(q_e-q_t)^2 \quad (3)$$

Where $K_{2,ads}$ is the rate constant for pseudo-second-order sorption . Integrating equation (3) with the boundary conditions q_t=0 at t=0 gives

$$t/q_t=t/q_e+1/K_{2,ads}\, q_e^2 \quad (4)$$

Thus, for pseudo-second-order kinetics a plot of t/q_t versus t should result in a straight line, with the values of q_e and $K_{2,ads}$ being determined from the slope and intercept. Figure 7 shows a plot to test such pseudo-second-order kinetics. The values of sorption rate constant, the equilibrium uptake and the correlation coefficient are listed in table 3.

As can be seen from figure 7 and table 3, pseudo-second-order kinetics gave a good fit to the data for the sorption of Fe (Ш) and Mn (П) onto the HNO_3 oxidized carbon C1.

The kinetic data obtained were also fitted to the intra particle diffusion model presented by the equation [43]

$$q_t = K_d t^{0.5} \quad (5)$$

where K_d is the rate constant for intra particle diffusion (mg/g. $min^{1/2}$). The subsequent linear plots of uptake against the square root of the contact time obtained are depicted in figure 8. A good correlation

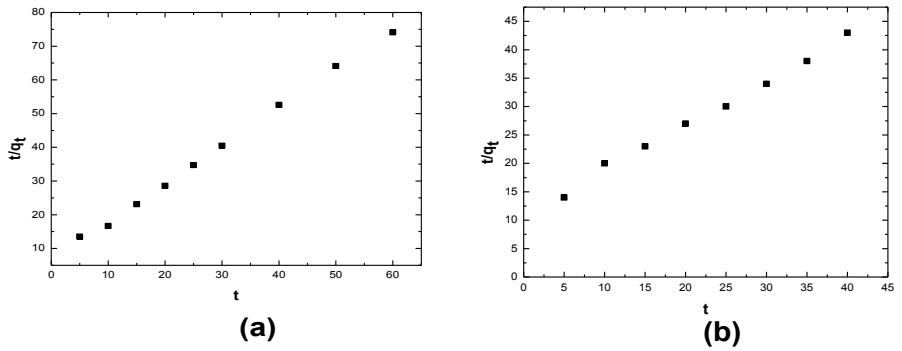

Figure 7: Linear plots of t versus t/q_t of a Fe(Ш) and b Mn(П) sorption at 25 °C on oxidized carbon C1.

Metal ion	Experimental	First-order model			Second-order model		
	$q_{e\,(exp)}$	$K_1(min^{-1})$	q_e(theor)(mg/g)	R^2	K^2(g/mgmin)	qe(theor)(mg/g)	R^2
Fe(Ш)	0.85	$3.67*10^{-1}$	0.273	0.81	$2.08*10^{-1}$	0.87	1
Mn(П)	1.25	$3.5*10^{-2}$	1.02	0.95	$8.25*10^{-2}$	1.21	1

Table 3: First-order and second-order constants for the adsorption of Fe (Ш) and Mn (П) by carbon C1.

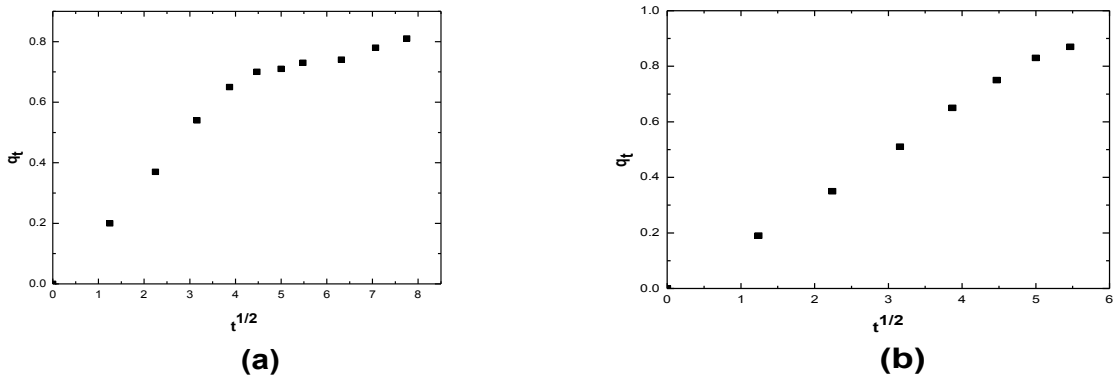

Figure 8: Linear plots of uptake against the square root of the contact time of (a) Fe(Ш) and (b) Mn (П).

coefficient for the experimental results with the linearized form of the model would indicate that the diffusion mechanisms are controlling factors in the sorption kinetics. Correlation coefficients were found to be very high, i.e R^2=1 for Fe (Ш) and Mn (П), respectively. The fact that the linear line passed through the origin and the linearity extended over a relatively wide range could indicate that intra particle diffusion is the only phenomenon occurring.

Effect of sorbent concentration: In this case, the effect of different amounts of sorbent on the removal of Fe (Ш) and Mn (П) was considered. Experiments were conducted using 50 ppm Fe (Ш) and 50 ppm Mn (П) at an initial pH 6 and different sorbent concentrations viz., 5,10,20,30 and 50 mg/L. The adsorption data for the residual concentration of Fe (Ш) and Mn (П) ions versus the amount of sorbent used are present in figure 9.

The results indicate that a greater amount of Mn^{2+} was removed from the solution with increasing amount of the sorbent in the system. This effect may be explained in terms of the availability of a greater surface area with a higher number of functional groups on the AC surface.

Effect of pH: The removal of heavy metal ions from aqueous solution is known to be strongly dependent on the pH value of the solution [44]. The solution pH affects the surface charge on the solid particles and the solubility of the metal ions. The effect of pH Fe (Ш) and Mn (П) adsorption by the HNO_3-oxidized carbon C1was studied over an initial pH range of 2-7. Figure 10 depict a plot for the uptake of Fe (Ш) and Mn (П), respectively as a function of initial pH of the solutions where the initial Fe (Ш) and Mn (П) concentrations were 5 ppm, adsorbent concentration 50 mg and adsorption solution volume 50 ml.

Effect of the solution volume: To determine the influence of the solution volume, the concentration of Fe (Ш) and Mn (П) was 5 ppm, the mass of the sorbent "carbon C1" was 50 mg, the initial pH 6. Figure 11 shows the metal ion uptake as a function of the volume of the adsorption solution. It is shown that for both metal ions, i.e Fe (Ш) and Mn (П), the metal ion uptake by carbon C1 decreased with the increase of the sorption solution volume. This may be explained by considering the increase of the thickness of the diffusion layer.

Equilibrium sorption of Fe (Ш) and Mn (П): The adsorption isotherms of Fe (Ш) and Mn (П) on ACs investigated are shown in figure 12. The isotherms are of Langmuir type, i.e type L with steep initial portion and with a plateau starting at relatively low concentration and covers a wide range of equilibrium concentrations.

The adsorption isotherms were analyzed using the linear form of the Langmuir equation, i.e., equation (6)

$$C_e/q_e = C_e/q_m + 1/K_{L.qm} \quad (6)$$

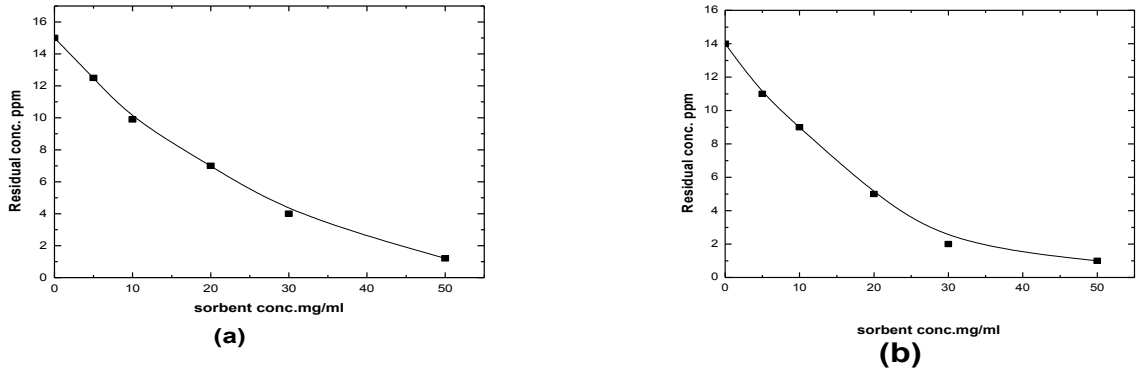

Figure 9: Influence of sorbent concentration "carbon C1" on the uptake of (a) Fe(Ш) and (b) Mn(П) from aqueous solution.

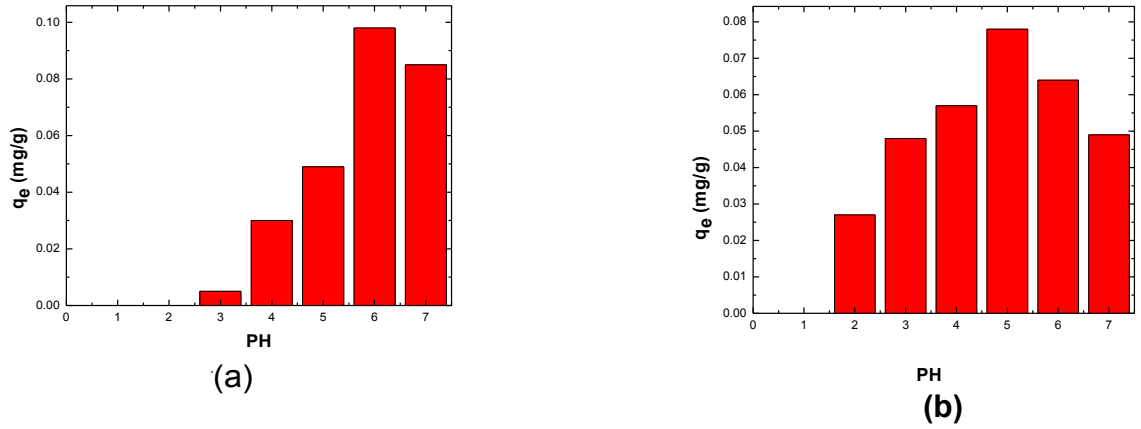

Figure 10: Uptake of (a) Fe(Ш) and (b) Mn(П) by "carbon C1" as a function of initial solution pH.

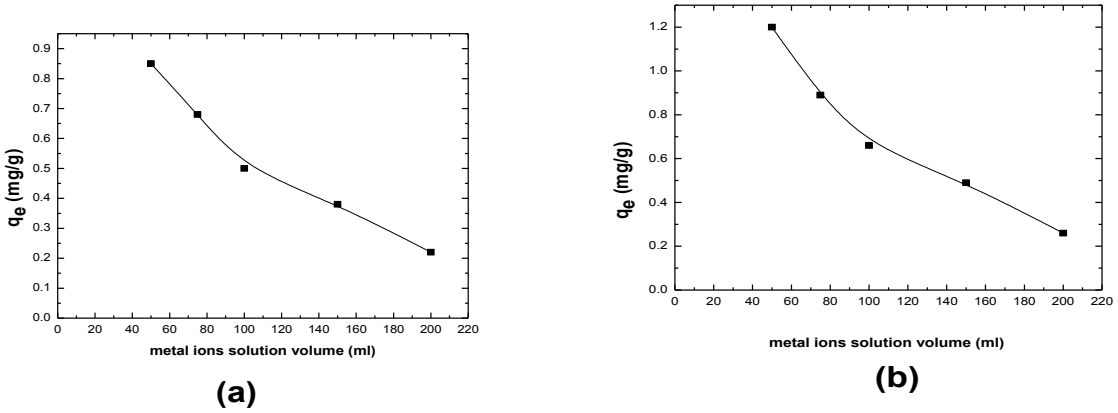

Figure 11: Influence of solution volume "carbon C1" on the uptake of (a) Fe(Ш) and (b) Mn(П) from aqueous solution.

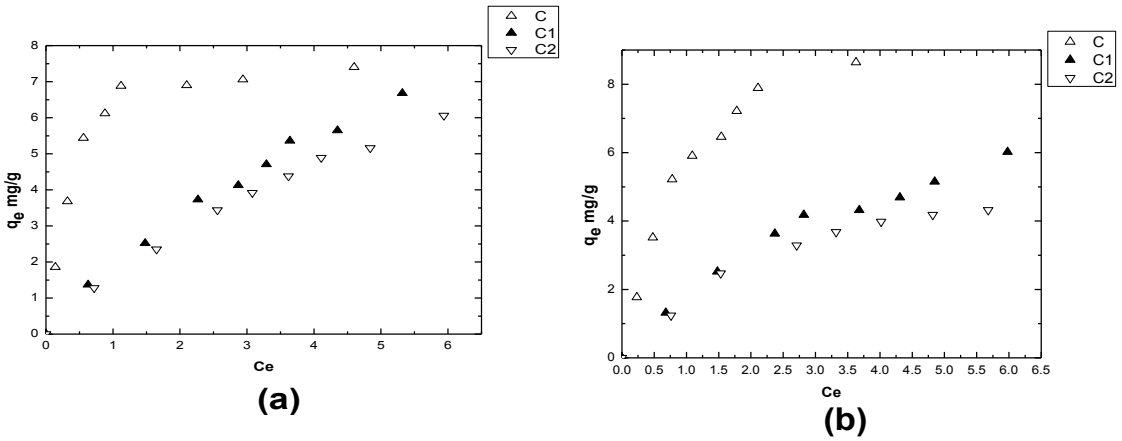

Figure 12: Equilibrium adsorption isotherms of (a) Fe(Ш) and (b) Mn(П) on C, C1 and C2.

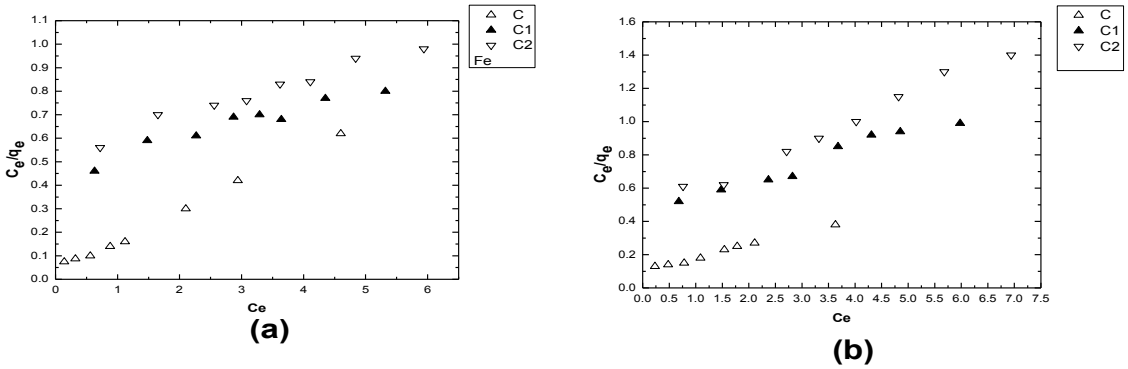

Figure 13: Linear Langmuir plots for equilibrium adsorption isotherms of Fe(Ш) and Mn(П) on C, C1 and C2.

Where q_e (ppm) is the amount adsorbed at equilibrium concentration C_e (ppm), qm (ppm) is the maximum sorption capacity, convention-ally considered as the mono layer capacity and K_L is the Langmuir adsorption constant (L/mg). The linear Langmuir plots of Fe (Ш) and Mn (П) adsorption on all the investigated carbons are shown in figure 13. Values of q_m and K_L are listed in table 4 together with the values of regression coefficients R^2 of each system. The high values of R^2 refer to the excellent fit of the results obtained to the Langmuir model.

Mechanism of adsorption

Modification of the carbon surface via oxidation with concentrated nitric acid introduces a variety of carbon oxygen functional groups of acidic nature. These groups dissociate in aqueous solutions and participate in the metal binding process. It is likely that other surface oxygen atoms (some of them may not be a component of protonogenic functional groups) may participate in metal complex formation. Thus,

Sample	Fe(Ш)		Mn(П)	
	q_m mg/g	K_L L/mg	q_m mg/g	K_L L/mg
C	8.06	2.07	9.52	1.62
C1	12.2	0.195	10	0.22
C2	10.64	0.192	6.66	0.38

Table 4: The values of q_m and K.

one would expect an ion exchange between Fe (Ш) and Mn (П) with the H^+ released from the carboxylic and phenolic surface groups and therefore these groups contribute significantly to the enhancement of metal ion uptake. Carbonyl and/or lactonic groups, on the other hand are more likely involved in a complex formation with metal ions like Fe (Ш) and Mn (П) [45].

Conclusion

The results obtained in this study clearly demonstrated the potential use of activated carbons derived from olive stones for the removal of Fe (Ш) and Mn (П) from aqueous solutions. The following conclusions can be drawn based on obtained results:

d. Nitric acid and persulphate-activated carbons possess polar surfaces due to the existence of a number of carbon-oxygen groups of different basicity.

e. The sorption of Fe (Ш) and Mn (П) ions onto chemically activated carbons is high and the mechanism of ion exchange is predominating.

f. The kinetic studies indicated that equilibrium in the adsorption of Fe (Ш) and Mn (П) on activated carbon was attained within one hour.

g. The optimum pH corresponding to the maximum adsorption was found to lie between 5.0 and 6.0.

h. The amount of Fe (Ш) and Mn (П) adsorbed increased with the increase of concentration

i. The extent of adsorption for Fe (Ш) and Mn (П) increased along with an increase of activated carbon dosage.

j. Pseudo-second-order kinetics gave a good fit to the data for the sorption of Fe (Ш) and Mn (П) into the HNO_3-activated carbon, and also the correlation coefficients for second-order model are higher than the first-order model for Fe (Ш) and Mn (П).

k. The high values of R2 in Langmuir model give an indication of favorable adsorption.

References

1. Giammanco S, Vatenza M, Pignato S, Giammanco G (1996) Mg, Mn, Fe and V concentrations in the ground water of Mount Etna (Sicity). Water Res 30: 378-386.
2. WHO (2003) Guidelines for Drinking Water Quality. World Health Organization, Germany.
3. Kontari E (1988) Groundwater, iron and manganese, an unwelcome trio. Water Eng Manag 25-26.
4. Komewska E, Lach J, Kacpzak M, Neeza E (2007) The removal of manganese, iron and ammonia nitrogen on impregnated activated carbon. Desalination 206: 251-258.
5. Takeda A (2003) Manganese action in brain function. Brain Res Rev 41: 79-87.
6. Donaldson J (1987) The physicopathlogic significance of manganese in brain. Neuro Toxicology 8: 451-462.
7. Bhattachayya D, Jumawan A, Sun G, Schwitzebel K (1980) Precipitation of sulphide: Bench Scale and Full scale experimental results. AICHE symposium series, Water 77: 31-42.
8. Linstedt KD, Houck CP, O'Connor JT (1971) Trace element removals in advanced waste water, treatment processes. J Water Pollut Control Fed 43: 1507-1513.
9. Daniels SL (1975) Removal of heavy metals by iron salts and polyelectrolytic flocculants. AICHE symposium series. Water 71: 265-271.
10. EPA (1987) Manual of treatment techniques for meeting the Interim primary drinking water regulations EPA600877005.
11. Knocke WR, Clevenger T, Ghosh MM, Novak JT (1978) Recovery of metals from electroplating waste waters. Proc. 33rd Purdue Industrial waste conf 33: 415-426.
12. McDonald CW, Bajwa RS (1977) Removal of toxic metal ions from metal finishing waste water by solvent extraction. Sep Sci 12: 435-445.
13. EPA (1979) Economic of waste water Treatment Alternatives for the Electroplating Industry. EPA 625/5-79-016.
14. Kim BM (1984) A membrane extraction process for selective recovery of metals AICHE Annual meeting, San Francisco, CA 26-30.
15. Muzzarelli R (1971) Application of polymers in marine ecology, Revue Int Oceanogr Med 21: 93-108.
16. Jellinek HHG, Sangel SP (1972) Complexation of metal ions with natural polyelectrolytes (removal and recovery of metal ions from polluted waters. Water Res 6: 305-314.
17. Dean JG, Bosqui FL, Lanoutte KH (1972) Removing heavy metals from waste water. Environ Sci Technol 6: 518-522.
18. Chang SY, Huang JC, Liu YC (1984) Heavy Metals Removal in affixed film biological system. Summer National AICHE meeting, Philadelphia PA 19-22.
19. Potterson JW, Minear RA (1975) Physical-chemical methods of heavy metal removal, in" Heavy Metals in Aquatic Environment. P.A. Krenkel, edn., Pergamon Press. Oxford, England 261-276.
20. De Mora SJ, Harrison RM (1983) The use of physical separation techniques in trace metal speciation studies. Water Res17: 723-733.
21. Cartwright PS (1981) Reverse osmosis and ultrafiltration in the plating shop. Plating Surf Fin 68: 40-45.
22. Youssef AM, El-wakil AM, El-Sharkawy WA, Farag AB, Toggan KH (1996) Adsorption of heavy metals on coal-based active carbons. Adsorpt Sci Technol 13: 115-124.
23. Youssef AM, Mostafa MR (1997) Removal of metal ions by modified activated carbon. J Appl Si 7: 1-15.
24. Youssefn AM, El-Nabarawy Th, Samra SE (2004) Sorption properties of chemically-Activated carbons. I. Sorption of Cd(11). Colloids and surfaces 235: 153-163.
25. Youssef AM, El-Nabarawy Th, El-shafey El (2006) Modified activated carbons from olive stones for removal of heavy metals. Carbon Science 6: 1-9.
26. Youssef AM, El-Khouly S, El-Nabarawy Th (2008) Removal of Pb(11) and Cd(11) from aqueous solution using activated carbons from pecan shells. Carbon Lett 9: 8-17.
27. Caturla F, Martin-Martinez JM, Molina-Sabio M, Rodriguez-Reinoso F, Torregrosa R (1988) Adsorption of substituted phenols on activated carbons. J Colloid Interface Sci 124: 528-534.
28. Alaya MN, Youssef AM, Karman M, Abdel-Al H (2006) Textural properties of activated carbons from wild cherry stones as determined by nitrogen and carbon dioxide Adsorption. carbon Sci 7: 9-18.
29. Youssef AM, Alaya MN, Nawar N (1994) Adsorption properties of Activated Carbons Obtained from Polymer wastes. Adsorp Sci Techol 11: 225.
30. Brunaur S, Emmett PH, Teller E (1938) Adsorption of Gases in Multimolecular Layers. J Am Chem Soc 60: 309-319.
31. Brunaur S, Deming LS, Deming WS, Teller E (1940) On a theory of the Vander Waals Adsorption of Gases. J Am Chem Soc 62: 1723-1732.
32. Sing KSW (1968) Chem Ind (London) 1520.

33. Sellez-Perez MJ, Martin-Martinez JM (1991) Classification of αs plots obtained from N2/77 K adsorption isotherms of activated. Fuel 70: 877-881.

34. Lodeirop, Barriada JL, Herrero R, Sastre de Vicente ME (2006) The marine macroalga cystoseira baccata as biosorbent for cadmium (П) and lead (П) removal: Kinetic and equilibrium studies. Environ Pollut 142: 264-273.

35. 35. Thrower PA (1989) Chemistry and physics of carbon. Marcel-Dekker, USA.

36. Karunakaran K, Thamilarasu P (2010) Removal of Fe (Ш) from aqueous solutions using Ricinus communis seed shell and polypyrrole coated Ricinus communis seed shell activated carbons. International Journal of Chem Tech Research 2: 26-35.

37. Shindo A, Izumino k (1994) Structural variation during pyrolysis of furfuryl alcohol and furfural-furfuryl alcohol resins. Carbon 32: 1233-1243.

38. Youssef AM, El-Khouly SM, El-Nabarawy Th (2008) Removal of Pb(II) and Cd(II) From Aqueous solution Using Oxidized Activated Carbons Developed From Pecan Shells. Carbon letters 9: 8-16.

39. Cox M, El-Shafey EI, Pichugin AA, Appeleton Q (1999) Preparation and characterization of a carbon adsorbent from flax shive by dehydration with sulfuric acid. Chem Technol Biotechnol 74: 1019-1029.

40. Gaid A, Kaoua F, Mederres N, Khodjsa M (1994) Surface mass transfer processes using activated date pits as adsorbent. Water SA 20: 273-278.

41. Asku Z (2001) Equilibrium and kinetic modeling of cadmium (II) biosorption by C. vulgaris in a batch system: effect of temperature. Sep Purif Technol 21: 285-294.

42. Ho YS, Mckay G (2000) The kinetics of sorption of divalent metal ions onto sphagnum moss peat. Water Res 34: 735-742.

43. Youssef AM, Mostfa MR (1992) Removal of copper ions by modified activated carbons. Indian J Technol 413.

44. Youssef AM, El-Nabarawy Th, SE Samra (2004) Sorption properties of chemically-Activated carbons. I. Sorption of Cd(11) ions. Collids and surfaces A 235: 153-163.

45. Jellinek HHG, Sangel SP (1972) Complexation of metal ions with natural polyelectrolytes (removal and recovery of metal ions from polluted waters). Water Res 63: 205.